NUEJ
NARESUAN UNIVERSITY
ENGINEERING JOURNAL

Adiabatic Temperature Change of Gadolinium Modeling using Artificial Neural Network

S. Jarungthammachote[1*], R. Prapainop[2]

Energy Systems Research Group, Faculty of Engineering at Sriracha, Kasetsart University, Sriracha Campus
[*] Corresponding author: sompop.j@ku.th
[2] E-mail: rotchana@eng.src.ku.ac.th

Abstract

An adiabatic temperature change of magnetocaloric material is an important parameter required in an active magnetic regenerator modeling. In this study, the adiabatic temperature change of Gadolinium was modeled by using artificial neural network. The adiabatic temperature changes were found at different magnetic inductions and magnetic material temperatures by means of WDS (Weiss-Debye-Sommerfeld) method. These data were applied to train a multilayer neural network with backpropagation algorithm. Artificial neural network with one hidden layer was chosen and the number of neurons was varied in training process until its mean square error (MSE) is lower than 10^{-6}. From the training result, the optimum number of neurons in the hidden layer is 16. Untrained data were used to test the optimum structure. It is found that MSE of testing is 4.46×10^{-5}. The weights and biases obtained from the optimum structure were used to model the adiabatic temperature change. Finally, an example code for the adiabatic temperature change calculation based on the weights and biases was presented as a guide for application.

Keywords: Adiabatic Temperature Change, Gadolinium, Neural Network, Active Magnetic Regenerator

1. INTRODUCTION

Magnetic refrigeration (MR) is an emerging technology without use of ozone depleting gases. The working concept of MR is based on the magnetocaloric effect (MCE) of magnetocaloric material, for example Gadolinium (Gd). MCE was discovered by Warburg in 1881 [1]. In 1976, Brown built the first magnetic heat pump operating at room temperature by applying magnetic induction of 7 Tesla to Gd [2]. Magnetocaloric effect can be simply explained as an adiabatic reversible change of magnetic material temperature under the variation of magnetic field. An increase of magnetic field applied to magnetic material causes a temperature increase in material. If the magnetic material is cooled down to the surrounding temperature, removing magnetic field can cause the temperature of magnetic material dropped below the surrounding temperature.

Magnetic refrigeration at room temperature has been interested by many researchers [1-4]. Active magnetic regenerator (AMR), one of the magnetic refrigerator designs, consists of a magnetocaloric material traversed by a fluid which flows from the cold end to the hot end of the regenerator [5]. To develop an AMR prototype, numerical modeling of the system is useful, because it saves budget and time for optimizing design under various operating conditions. Several AMR models have been published in the literatures [6-13]. Since the magnetocaloric properties of Gd are widely published, Gd has become the reference magnetocaloric material in the scientific community. Then, in both numerical and experimental studies of AMR, Gd has been often used.

Presenting MCE of magnetocaloric material in the model, this is an important step which is quite complex. In literatures, the MCE can be considered in the model by two approaches. The first one is using derivative of thermodynamic property of the magnetocaloric material, referred as built-in method [9]. Researches using built-in method have been found in [5, 7, 10, 11]. The second method is applying adiabatic temperature change (ΔT_{ad}) directly into the model, called discrete method [12, 15]. Nielsen et al. [9] reported that the discrete method is the simplest and most straightforward way, while the built-in method requires details and numerically differentiable data of magnetization and specific heat as function of both temperature and magnetic field. Use of the adiabatic temperature change in magnetic refrigerator model can be found in [6, 8, 12, 15].

To find the adiabatic temperature change value, WDS (Weiss-Debye-Sommerfeld) method, explained in the next section, is usually performed. However, WDS method significantly consumes time and computer resources. Most of AMR models are often developed by finite difference method. Calculation of adiabatic temperature changes in all nodes can cause large computational delay. The better way to find the adiabatic temperature change is using the adiabatic temperature change equation which is formed as a function of magnetic induction, B, (or magnetic field strength, H depending on the information that user has) and magnetic material temperature.

Siddikov et al. [6] presented the adiabatic temperature change equation of Gd by using the least-squares fitting technique and experimental measurements. In other words, the least square technique they applied requires some constants, obtained from numerical experiments. However, the experimental data used to fit the equation are not shown in their published paper. Furthermore, after further investigated by the authors, it is found that, at some magnetic inductions, their equation gives unreasonable values of the adiabatic temperature change.

Artificial neural network or neural network is a technique widely used to mimic properties of material, [16-18]. The aim of this work is to develop a mathematical model of the adiabatic temperature change related to magnetic induction and magnetic material temperature for Gd by means of neural network. In this

work, we are interested to use the WDS method to find the adiabatic temperature changes of Gd. The data obtained from WDS method are adopted to train the neural network in order to generate a mathematical model for the adiabatic temperature change of Gd, relating to the magnetic induction and the magnetic material temperature.

The developed adiabatic temperature change model should be simple to construct a computer program, because it is often used in AMR model. In this paper, the MCE is discussed and the WDS method is shown in section 2. Then, the calculated adiabatic temperature changes at different magnetic inductions and material temperatures are obtained. In section 3, the neural network method, used to find the relationship between magnetic induction, metrical temperature and the adiabatic temperature change, is discussed. The results of neural network training and testing are shown. Finally, an example code for computing the adiabatic temperature change is presented.

2. SIMULATION OF THE MAGNETOCALORIC EFFECT

In a numerical study of AMR, the adiabatic temperature change is one of the most important parameters needed to be known. Especially, in the AMR model called the discrete method, the magnetocaloric effect in the model is to apply the adiabatic temperature to the solid during the magnetization and demagnetization periods directly [9] . To find the adiabatic temperature change, WDS model is often used. However, before WDS model is described, the magnetocaloric effect should be further explained.

The temperature-total entropy diagram of magnetic material is shown in Fig.1. At constant pressure, the entropy of magnetic material is a function of magnetic field strength, H (or magnetic induction, B , depending on the parameter wanted to present) , and temperature, T or $S(H,T)$. For initial temperature of T_o and magnetic field strength of H_o , the total entropy of magnetic material is $S_o(H_o,T_o)$. If the applied magnetic field strength is changed to H_1 with adiabatically reversible process, the total entropy of magnetic material remains constant or $S_1 = S_o$. Therefore, the new equilibrium state is at $S_1(H_1,T_1)$. In Fig.1, the magnetic field strength H_o is zero and $H_1 > H_o$ ($\Delta H > 0$) . Therefore, $\Delta T_{ad}(\Delta H,T)$ is positive. Nevertheless, $\Delta H < 0$, $\Delta T_{ad}(\Delta H,T)$ is negative. Further explanation on the magnetocaloric effect is shown by [19].

As explained, the total entropy of magnetic material is required to find the adiabatic temperature change. The following shows the WDS model and other principles utilized to find the total entropy, consequently, the adiabatic temperature change is obtained.

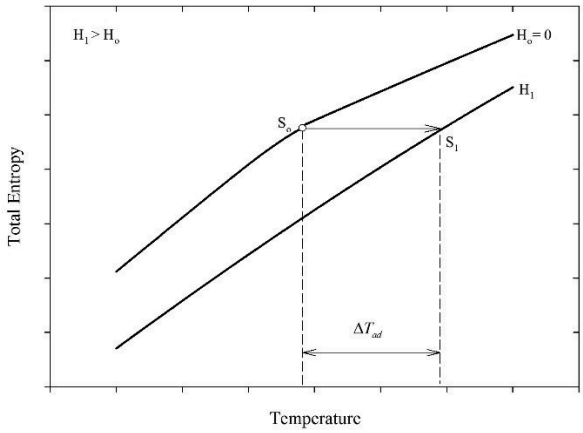

Figure 1 T-S diagram of magnetic material

2.1 The Weiss mean field theory

A magnetic entropy, S_m , is a part of total entropy. Based on the Weiss mean field theory, Tishi [20] showed that the magnetic entropy is given as:

$$S_m(B,T) = N_A k_B \left[\ln\left(\frac{\sinh\left(\frac{2J+1}{2J} X \right)}{\sinh\left(\frac{X}{2J} \right)} \right) - X B_J(X) \right] \quad (1)$$

where N_A is the Avogadro's number and k_B represents the Boltzmann constant. However, the term in front of square bracket can be $N_A k_B / MW$ where MW is molar mass [12, 8]. This term depends on the unit of entropy required. de Oliveira et al. [21] suggested that this term can be replaced by N which is the number of magnetic atoms per unit formula (per kg or per mol) . In Eq. (1), $B_J(X)$ denotes the Brillouin function, defined as:

$$B_J(X) = \frac{2J+1}{2J} \coth\left(\frac{(2J+1)X}{2J} \right) - \frac{1}{2J} \coth\frac{X}{2J} \quad (2)$$

where J represents the total angular momentum and X is given as following [21]

$$X = \frac{g_J \mu_B B J}{k_B T} + \frac{3 T_c B_J(X) J}{T(J+1)} \quad (3)$$

where g_J denotes the spectroscopic splitting factor and μ_B is the Bohr magneton. B and T_c are the magnetic induction and the Curie temperature, respectively. Since the magnetic induction, B relates to magnetic field strength, H . Even the previous details were discussed in terms of magnetic field strength, the magnetic induction can be used instead of H in here and after.

To find the value of magnetic entropy, Eqs. (2) and (3) are simultaneously solved by numerical method. In this study, Eq. (3) was rearranged to present $B_J(X)$ as a function of other parameters and this new equation is set to be equal to Eq. (2). The numerical technique called bisection method is applied to find the value of X and then $B_J(X)$ is found by substituting X into Eq. (2).

Finally, the magnetic entropy can be obtained from Eq. (1).

Before other entropies are explained, it is worth to discuss more about solving Eqs. (2) and (3). Fig. 2 illustrates the solution, $B_J(X)$, solved from both equations at different temperatures. The solid lines in Fig.2 are $B_J(X)$ calculated from Eq. (3) for different cases of temperature and the dash line is $B_J(X)$ computed from Eq. (2). All lines in Fig. 2 are determined based on the parameters ($J, T_c, ...etc.$) associated with Gd. The lower value of magnetic induction (B = 0.5Tesla) is used for plotting Fig. (2). However, if higher value of B is applied to Eq. (3), $B_J(X)$ at lower value of X is negative. The intersection of both lines (solid and dash lines) is the solution. From Fig.2, it is clearly seen that at $T = T_c$ and $T > T_c$ the solution is approaching to zero. For $T < T_c$, the solution has higher value than the previous cases. It should be noted here that for $T > T_c$ and $T = T_c$, if higher value of B is substituted into Eq. (3), the solution must have higher value than that expressed in Fig. 2

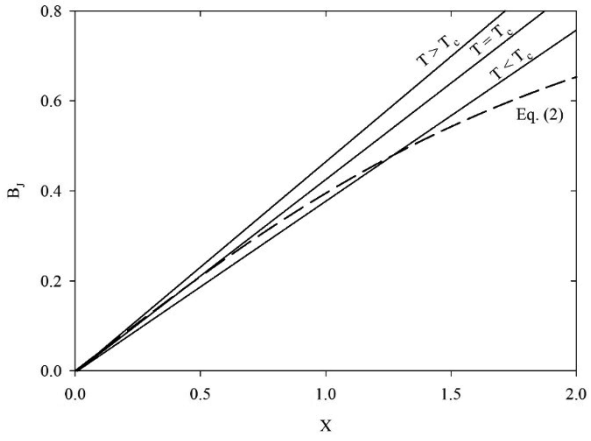

Figure 2 Solutions of Eqs. (2) and (3) at different temperatures

2.2 The Debye theory

The lattice contribution to the specific heat implies the lattice contribution to the entropy, S_l, as [22]:

$$c_{v,l} = T\left(\frac{\partial S}{\partial T}\right)_{\theta_D} \tag{4}$$

Kittel [23] showed that:

$$c_{v,l} = 9N_A k_B \left(\frac{T}{\theta_D}\right)^3 \int_0^{\theta_D/T} \frac{x^4 e^x}{\left(e^x - 1\right)^2} dx \tag{5}$$

where θ_D is the Debye temperature. Substituting Eq. (5) to Eq. (4), the lattice entropy is determined as:

$$S_l(T) = N_A k_B \left[\begin{array}{l} -3\ln\left(1 - e^{-\theta_D/T}\right) + \\ 12\left(\frac{T}{\theta_D}\right)^3 \int_0^{\theta_D/T} \frac{x^3}{\left(e^x - 1\right)^2} dx \end{array} \right] \tag{6}$$

The integration term of Eq. (6) can be obtained by using trapezoidal rule.

2.3 The Sommerfeld theory

Ashcroft and Mermin, [24] have discussed about the Sommerfeld theory of conduction in metals. They summarized that the heat capacity per unit mole contributed by free electron is:

$$c_e = \gamma T \tag{7}$$

This relation is also found in Callen [22]. The coefficient, γ, for some metals obtained from calculation compared with measurement are shown in [24]. According Eq. (4), the entropy of electron can be obtained as:

$$S_e(T) = \gamma T \tag{8}$$

2.4 Total entropy

The total entropy, which is a function of temperature and magnetic induction, is the sum of the three entropies or:

$$S(B,T) = S_m(B,T) + S_l(T) + S_e(T) \tag{9}$$

To find the adiabatic temperature change in magnetization process, a numerical method, called secant method, is employed. The iterative equation, which is developed from this method, is [25]:

$$x_{i+1} = x_i - \frac{f(x_i)(x_{i-1} - x_i)}{f(x_{i-1}) - f(x_i)} \tag{10}$$

For this problem, x is the temperature of magnetic material in adiabatic magnetization state and subscript i indicates the number of iterations. $f(x_i)$ represents $S(B_o,T_o) - S(B_1,T_i)$. The calculation program is terminated when $f(x_i) < 10^{-6}$ and the solution is referred as T_1. The adiabatic temperature change is $\Delta T_{ad} = T_1 - T_o$.

The adiabatic temperature change was calculated following WDS method. Before the calculated adiabatic temperature changes are used to train the neural network, some calculated results are validated with the data from [26, 27]. In this study, the magnetic induction is varied from 0.5Tesla to 10Tesla with incremental of 0.25Tesla, while the magnetic material temperature is increased from 230K to 330K with incremental of 1K. The adiabatic temperature change is calculated and it is used to train a neural network. Therefore, the training data is, then, totally 3939.

3. DESIGN AND TRAINING OF AN ARTIFICIAL NEURAL NETWORK

In this research, the multilayer perceptron network (MLPN) with backpropagation algorithm was used to predict the adiabatic temperature change of Gd. The number of hidden layers and the number of neurons or nodes in each hidden layer are flexibly chosen. However, to have optimum neural network structure, some criterions and recommendations from previous researches are adopted in this work.

Christodoulou and Georgiopoulos [28] has mentioned that MLPN with one hidden layer and nonlinear activation functions for the hidden nodes can implement any function of practical interest. The agreement with the above discussion is also found in work of Azizi et al. [29]. The objective of this research is to develop a simple mathematical model to find the adiabatic temperature change of Gd, therefore, the MLPN, consisting of one input layer, one hidden layer, and one output layer, is selected, as shown in Fig 3.

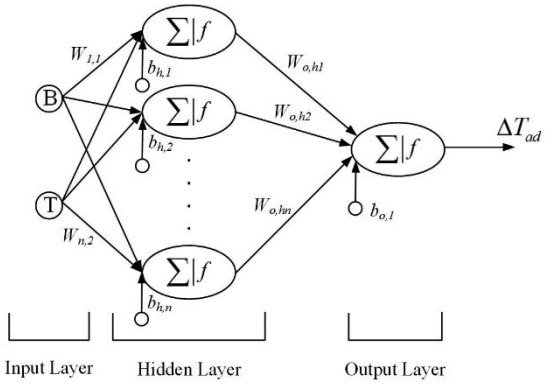

Figure 3 Chosen MLPN structure

In Fig. 3, the symbols W and b represent weight and bias, respectively. f shown in hidden and output layers is transfer function (also called activation function [30]). The number of neurons in hidden layer is not yet known and it is defined as n. In this work, there are two inputs, the magnetic induction, B and magnetic material temperature, T. The inputs multiply with connection weights. The multiplication is summed with biases and the summation result goes into transfer function and produces neuron output. The neuron outputs from hidden layer are treaded as input to the output layer. The similar procedures are carried out in output layer, which has only one neuron, and the network output, ΔT_{ad} is obtained. The equation used to explain the above process is:

$$\Delta T_{ad} = f_o(W_{o,hn} f_h(W_{n,i} X_i + b_{h,n}) + b_{o,1}) \tag{11}$$

where X_i is input vector and $i = 1, 2$.

As found in [16-18, 26, 29], the transfer function applied in the hidden layer is nonlinear and there are hyperbolic tangent and log sigmoid transfer functions. Liu et al. [31] mentioned that the hyperbolic tangent transfer function is the most commonly used in hidden layer. For output layer, the linear transfer function is often used. Thus, in this research, hyperbolic tangent transfer function is applied in the hidden layer and linear transfer function is used in the output layer.

Backpropagation is well known to be the most widely applied to train the MLPN. It involves two stages, feed-forward stage and error backpropagation. In the error backpropagation, the weights and biases are improved to obtain some desired outputs. Levenberg-Marquardt learning algorithm is employed in this study. The network errors taking place during training process can be expressed in terms of mean square error (*MSE*) and it is defined as:

$$MSE = \frac{1}{k}\sum_{j=1}^{k}\left(y_j - o_j\right)^2 \tag{12}$$

where y and o are target output and network out, respectively and k is the number of data. In this work, accepted *MSE* is set to be 10^{-6}. The maximum number of training cycles or epochs is 1000. At the certain number of neurons, *MSE* is observed. If *MSE* is higher than the accepted *MSE* , the number of neurons in hidden layer is increased. Then, the training process is continued and *MSE* is checked. This procedure is repeated until *MSE* is lower than the accepted *MSE* . For the data used in the training process, these are generated from the WDS method previously explained. There are 3939 data for training and 966 untrained data are generated for testing. The outputs, ΔT_{ad} , are normalized between 0 and 1 by diving all outputs data by maximum ΔT_{ad} , which is 19.60118K.

4. RESULTS AND DISCUSSION

Table 1 presents the training results at different numbers of neurons in the hidden layer. In the table *MSE* values and coefficients of determination are shown for each case of neural network structures. It is found that, in 1000 epochs, the network with 16 neurons in the hidden layer can provide *MSE* value lower than 10^{-6}. The coefficient of determination) R^2 (is about 1. Moreover, the number of neurons is increased and the training process continues. It is found that *MSE* of training is still lower than 10^{-6}. To have the simple model to find the adiabatic temperature change, neural network structure with 16 neurons in hidden layer is firstly focused. To make sure that this neural network structure can generally predict the adiabatic temperature change even there are not trained adiabatic temperature change data. Therefore, the testing process is conducted and the *MSE* and R^2 are observed. 966 untrained data introduce to 2-16-1 neural network. The network output is compared to the actual output. The testing result is shown in Table 2. Besides the testing result of 2-16-1 network, Table 2 also presents testing results of other structures.

Table 1 The performance results of the network trainings for different numbers of neurons in the hidden layer

NO. of neuron in the hidden layer	*MSE*	R^2
1	1.17×10^{-2}	0.88753
2	8.60×10^{-4}	0.99218
3	2.79×10^{-4}	0.99747
4	7.35×10^{-5}	0.99933
5	7.95×10^{-5}	0.99928
6	4.15×10^{-5}	0.99962
7	4.41×10^{-5}	0.99960
8	2.33×10^{-5}	0.99979
9	1.16×10^{-5}	0.99989
10	5.92×10^{-6}	0.99995
11	4.90×10^{-6}	0.99996
12	5.88×10^{-6}	0.99995
13	2.46×10^{-6}	0.99998
14	5.77×10^{-6}	0.99995
15	1.09×10^{-6}	0.99999
16	$\boldsymbol{9.99\times10^{-7}}$	***0.99999***
17	9.99×10^{-7}	0.99999
18	9.98×10^{-7}	0.99999
19	9.80×10^{-7}	0.99999
20	9.99×10^{-7}	0.99999

Table 2 The performance results of testing process

Neural network structure	*MSE*	R^2
2-16-1	4.46×10^{-5}	0.99999
2-17-1	4.86×10^{-5}	0.99999
2-18-1	4.68×10^{-5}	0.99999
2-19-1	4.83×10^{-5}	0.99999
2-20-1	4.78×10^{-5}	0.99999

From Table 2, it can be observed that 2-16-1 network provides the lowest *MSE* value with R^2 of 1. Comparing to other structures expressed in this table, the *MSE* values are insignificantly different. Therefore, the network structure of 2-16-1 is selected as it is simple and gives lowest *MSE* . However, it should be mentioned here that the *MSE* values shown in Table 2 are calculated based on the normalized value of the adiabatic temperature change. For the actual value of the adiabatic temperature change, the network output has to be multiplied with 19.60118K. Thus, the *MSEs* , which are calculated based on the actual adiabatic temperature change are, of course, higher than that presented in Table 2. In the case of 2-16-1 network, the *MSE* value computed based on the actual adiabatic temperature change is 0.0171 with R^2 of 1. Fig. 4 presents the adiabatic temperature change calculated from WDS method discussed in section 2, called actual value, via the adiabatic temperature change calculated from 2-16-1 network, called predicted value. From the figure, it confirms that the adiabatic temperature change predicted from the 2-16-1 network is acceptable with average absolute relative error of 0.47%.

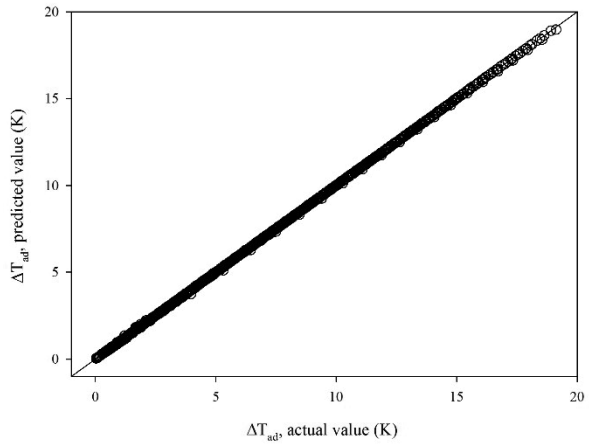

Figure 4 Comparison of ΔT_{ad} between actual values and predicted values from 2-16-1 network

To develop a mathematic model of the adiabatic temperature change at different magnetic inductions and temperatures, which is the objective of this research, the connected weights and biases, adjusted from training process, are required. The weights and biases are finally used to form the adiabatic temperature change model. For selected structure, the weights and biases are shown in Table 3. The weight, $W1$, is 2-dimensional array, while $b1$ and $W2$ are column matrix. Although, there are totally 65 constants)weights and biases(, it is simple to develop a computer code to calculate the adiabatic temperature change, as following MATLAB code.

```
function DTadNN=ApplCode(B,T)
load WB % WB=[W1, b1, W2, b2] shown in Table 3
NN=0;
for i=1 to 16
   n=tanh(WB(i,1)*B+WB(i,2)*T+WB(i,3))*WB(i,4));
   NN=n+NN;
end
DTad=(NN+WB(1,5))*19.60118
```

For the weights and biases, the researchers can copy from soft copy of this paper and paste into their computer codes. These weights and biases must be rearranged following the syntax of a computer language that the researches use. Generally, using WDS model to find the adiabatic temperature change consumes 15,600 μs while the developed model in this research (using the MATLAB code and constants in Table 3) spends 12 μs .

Finally, the developed model with the weights and biases are implemented to find the adiabatic temperature changes at different magnetic inductions and temperatures. Figure 5 shows the comparison of the adiabatic temperature change obtained from the developed model and WDS model. It obviously presents that the adiabatic temperature change from the developed model (Fig. 5(a)) completely match with that from WDS model (Fig. 5(b)).

Table 3 The connected weights and biases of 2-16-1 network

$W1(i,1)$	$W1(i,2)$	$b1(i)$	$W2(i)$	$b2$
1.4376E-01	8.3950E-02	-3.7284E+01	3.1092E-01	0.400739
-2.1090E+00	7.9854E-02	-2.2111E+01	-1.6217E-02	0
-1.3800E-01	-2.1936E-02	7.9901E+00	-1.2137E-01	0
1.2450E-01	-2.8263E-02	7.2124E+00	4.0868E+00	0
-1.4354E-01	3.2014E-02	-8.0583E+00	5.6434E+00	0
1.6328E-01	-3.5899E-02	8.9494E+00	2.0796E+00	0
5.8103E-02	5.5223E-02	-1.6188E+01	2.4148E-01	0
8.6532E-03	1.5991E-01	-4.7109E+01	3.5910E-01	0
8.5968E-03	1.7742E-01	-5.2416E+01	-3.4464E-01	0
-1.3861E-01	-4.2658E-02	1.2214E+01	-1.6077E-01	0
-2.7788E-01	-6.5912E-02	1.6671E+01	9.9687E-02	0
4.9556E-01	-6.9735E-02	1.9770E+01	4.5177E-02	0
1.7144E-01	3.7235E-02	-9.2525E+00	3.7098E-01	0
3.1908E-02	-9.1030E-02	2.7260E+01	9.0342E-02	0
-9.8330E-01	8.3555E-02	-2.3846E+01	-3.6534E-02	0
-3.5379E-01	-1.0835E-01	2.5832E+01	4.0205E-02	0

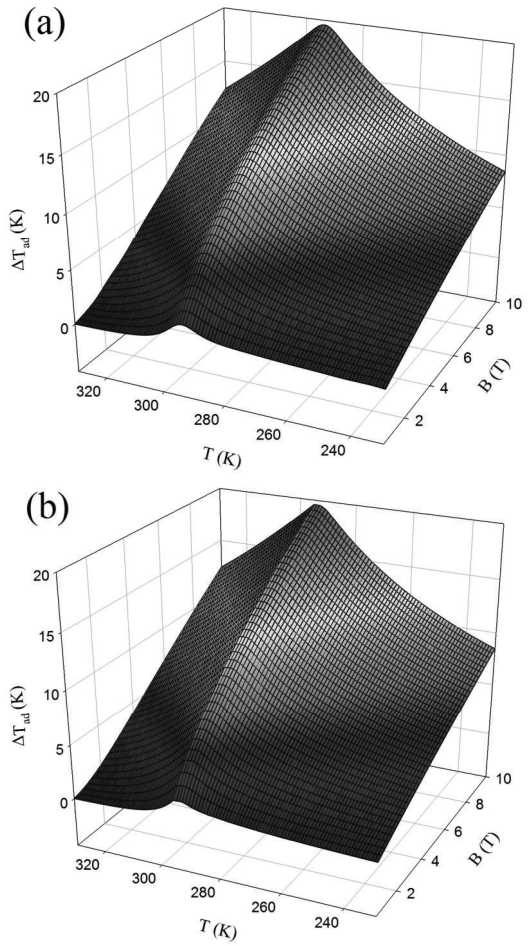

Figure 5 The surface of adiabatic temperature change of Gd (a) from 2-16-1 neural network, (b) from WDS method

5. CONCLUSION

In the present work, a mathematical model for the adiabatic temperature change related to magnetic induction and magnetic material temperature was developed by using neural network. The adiabatic temperature change obtained from WDS method was employed to train the neural network. The result of training process showed that the optimum neural network structure was 2-16-1. Hyperbolic tangent and linear transfer functions were applied as transfer functions in the hidden layer and the output layer, respectively. From the testing process, it showed that the mean square error was 0.0171 with R^2 of 1. The model of the adiabatic temperature change, obtained from network weights and biases, can be easily developed by computer program. For further research, SMV or genetic algorithm is recommended to use and its performance should be compared with that of neural network method.

6. ACKNOWLEDGMENT

The authors gratefully acknowledge the financial support from Faculty of Engineering at Sri Racha, Kasetsart University, Sri Racha Campus.

7. REFERENCES

[1] Gschneidner, K.A., & Pecharsky, K.V.)2008(. Thirty years of near room temperature magnetic cooling: Where we are today and future prospects. International Journal of Refrigeration, 31(6), 945–961. [2] Brown, G.V.)1976(. Magnetic heat pumping near room temperature. Journal of Applied Physics, 47, 3673–3680.

[3] Yu, B., Liu, M., Egolf, P.W., & Kitanovski, A.)2010(. A review of magnetic refrigerator and heat pump prototypes built before the year 2010. International Journal of Refrigeration, 33(6), 1029-1066.

[4] Lei, T., Engelbrecht, K., Nielsen, K.K., & Veje, C.T.) 2017(. Study of geometries of active magnetic regenerators for room temperature magnetocaloric refrigeration. Applied Thermal Engineering, 111(25), 1232–1243.

[5] Torregrosa-Jaime, B., Corberan, J. M., Paya, J., &Engelbrecht, K.)2015(. An efficient numerical scheme for the simulation of parallel-plate active magnetic regenerators. International Journal of Refrigeration, 58, 121-130.

[6] Siddikov, B.M., Wade, B.A., & Schultz, D.H.)2005(. Numerical simulation of the active magnetic regenerator. Computers and Mathematics with Applications, 49(9-10), 1525-1538.

[7] Engelbrecht, K.L., Nellis, G.F., & Klein, S.A.)2006(. Predicting the performance of an active magnetic regenerator used of space cooling and refrigeration. HVAC & Research, 2)4), 1077- 1095.

[8] Aprea, C., & Maiorinoi, A.)2010(. A flexible numerical model to study an active magnetic refrigerator for near room temperature applications. Applied Energy, 87(8), 2690-2698.

[9] Nielsen, K.K., Tusek, J., Engelbrecht, K., Schopfer, S., Kitanovski, A., Bahl, C.R.H., Smith, A., Pryds, N., & Poredos, A.)2011(. Review on numerical modeling of active magnetic regenerators for room temperature applications.International Journal of Refrigeration, 34(3), 603-616.

]10[Li, J., Numazawa, T., Nakagome, H., & Matsumoto, K.)2011(. Numerical modeling on a reciprocating active regenerator refrigeration in room temperature. Cryogenics, 51(6) 347-352.

]11[Park, I., Kim, Y., & Jeong, S.)2013(. Development of the tandem reciprocating magnetic regenerative refrigerator and numerical simulation for the dead volume effect. International Journal of Refrigeration, 36(6), 1741-1749.

]12[Trevizoli, P.V., Barbosa, J.R., Tura, A., Arnold, D., & Rowe, A.)2014(. Modeling of thermomagnetic phenomena in active magnetocaloric regenerators. Journal of Thermal Science and Engineering Applications, 6)3(, 0310161- 03101610.

]13[You, Y., Yu, S., Tian, Y., Luo, X., & Huang, S.)2016(A numerical study on the unsteady heat transfer in active regenerator with multi-layer refrigerants of rotary magnetic refrigerator near room temperature. International Journal of Refrigeration, 65, 238-249.

]14[Tusek, J., Kitanovski, A., Zupan, S., Prebil, I., & Poredo, A. (2013). A comprehensive experimental analysis of gadolinium active magnetic regenerators. Applied Thermal Engineering, 53)1(, 57-66.

]15[Kamran, M.S., Sun, J., Tang, Y.B., Chen, Y.G., Wu, J.H., & Wang, H.S. (2016). Numerical investigation of room temperature magnetic refrigerator using microchannel regenerators. Applied Thermal Engineering, 102)5(, 1126-1140.

[16] Bhattacharjee, D., & Kothari, V., (2007). A neural network system for prediction of thermal resistance of textile fabrics. Textile Research Journal, 77)1(, 4-12.

[17] Esfe, M.H., Wonswises, S., Naderi, A., Asadi, A., Safaei, M.R., Rostamian, H., Dahari, M., & Karimipour, A. (2015). Thermal conductivity of Cu/TiO2-Water/EG hybrid nanofluid: Experimental data and modeling using artificial neural network and correlation. International Communications in Heat and Mass Transfer, 66, 100-104.

[18] Singh, R., Bhoopal, R.S., & Kumar, S. (2011). Prediction of effective thermal conductivity of moist porous materials using artificial neural network approach. Building and Environment, 46(12), 2603-2608.

[19] Pecharsky, K.V., & Gschneidner, K.A. (1999). Magnetocaloric effect and magnetic refrigeration. Journal of Magnetism and Magnetic Materials, 200(1–3), 44-56.

[20] Tishi, A.M. (1990). Magnetocaloric effect in strong magnetic fields. Cryogenics, 30(2), 127-136.

[21] de Oliveira, N.A., von Ranke, P.J., & Troper, A. (2014). Magnetocaloric and barocaloric effects: theoretical description and trends. International Journal of Refrigeration, 37, 237-248.

[22] Callen, H.B. (1960). Thermodynamics: an introduction to the physical theories of equilibrium thermostatics and irreversible thermodynamics. Singapore: John Wiley & Son.

[23] Kittel, C. (2005). Introduction to solid state physics. (8th ed.). USA: John Wiley & Sons.

[24] Ashcroft, N.W., & Mermin, N.D. (1976). Solid state physics. USA: Harcourt Brace College Publishing.

[25] Chapra, S.C., (2005). Applied numerical methods with MATLAB for engineers and scientists. Singapore: McGraw Hill.

[26] Pertersen, T.F. (2007). Numerical modelling and analysis of a room temperature magnetic refrigeration system. (Ph.D. Thesis, The Technical University of Denmark).

[27] Yui, K. (2015). Development of a magnetocaloric heat circulator based on self-heat recuperation technology. (Ph.D. Thesis, University of Tokyo).

[28] Christodoulou, C., & Georgiopoulos, M. (2001).Applications of neural networks in electromagnetics. USA: Artech House.

[29] Azizi, S., Ahmadloo, E., & Awad, M.M. (2016). Prediction of void fraction for gas-liquid flow in horizontal, upward and downward inclined pipes using artificial neural network. International Journal of Multiphase Flow, 87, 35-44.

[30] Hagen, M.T., Demuth, H.B., & Beale, M. (1996). Neural network design. Boston, USA: PWS Publishing Company.

[31] Liu, N., Yang, H., Li, H., Yan, S., Zhang, H., & Tang, W. (2015). BP artificial neural network modeling for accurate radius prediction and application in increment in-plane bending. The International Journal of Advanced Manufacturing Technology, 80(5), 971-984.

8. BIOGRAPHIES

Dr. Sompop Jarungthammachote is an assistant professor in Mechanical Engineering at Faculty of Engineering at Sriracha, Kasetsart University, Sriracha Campus. His research interest is thermodynamic modeling of gasification and thermal systems.

Dr. Rotchana Prapainop is an assistant professor in Mechanical Engineering at Faculty of Engineering at Sriracha, Kasetsart University, Sriracha Campus. Her research interests are performance analysis of refrigeration and air conditioning systems and not-in-kind technologies for refrigeration and energy systems